Aerosol release fraction by concrete scarifying operations and its radiological impacts on the dismantling of nuclear facilities

Mamadou Sow, Yohan Leblois, Cecile Bodiot, Charles Motzkus, Sebastien Ritoux, Francois Gensdarmes

Journal Pre-proof

Aerosol release fraction by concrete scarifying operations and its implications on the dismantling of nuclear facilities

Mamadou Sow, Yohan Leblois, Cécile Bodiot, Charles Motzkus, Sébastien Ritoux, François Gensdarmes
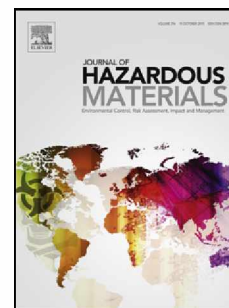
Please cite this article as: { doi: https://doi.org/

Aerosol release fraction by concrete scarifying operations and its implications on the dismantling of nuclear facilities

Mamadou Sow[1], Yohan Leblois[1], Cécile Bodiot[1], Charles Motzkus[2], Sébastien Ritoux[2] and François Gensdarmes[1]

[1]Institut de Radioprotection et de Sûreté Nucléaire (IRSN), PSN-RES, SCA, LPMA, Gif-sur-Yvette cedex, 91192, France
[2]Centre Scientifique et Technique du Bâtiment (CSTB), Division Agents Biologiques et Aérocontaminants, 84 Avenue Jean Jaurès, 77420 Champs-sur-Marne

Highlightd

- Airborne release of hazardous material associated with the sanitation of concrete.
- Concrete of nuclear installations experience activation due to the neutron flux.
- Industrial milling machine equipped with dust mitigation vacuum system.
- Aerosol produced is for 45 % in the respirable and for 82 % in the thoracic fraction.
- The mineralogical composition is dominated by calcium and silica.

Abstract:
The sanitation of concrete structures through dismantling of nuclear buildings is complicated by the radiological threat associated with the airborne release of fine dust. This is the reason why the aerosol release fraction (ARF) associated with mechanical removal of concrete structure containing radioactivity needs to be accurately evaluated to implement efficient radiological survey and containment techniques. We characterize experimentally the ARF resulting from milling operations on a standard non-radioactive concrete slab in a confined experimental chamber using an industrial scarifying machine. Our results reveal a significant production of fine aerosol particles with a mass median aerodynamic diameter close to 4 μm and which mineralogical composition is dominated by calcium and silica compounds. The ARF measured when a vacuum suction device is used to confine the dust production close to the source is on the order of 5×10^{-4}; the maximum ARF estimated when no suction device is used is on the order of 0.5. As the study is focused on non-radioactive concrete, transposition of aerosol characteristics investigated in this study to assess radioactive airborne release is only relevant for in-depth neutron activation on elemental compounds of concrete.
Keywords: Dismantling, airborne release, concrete, scarifying, aerosol
Corresponding author: mamadou.sow@irsn.fr

1 - Introduction

All over the running period of nuclear plants and laboratories, their concrete structures are activated by the neutron flux they undertake repetitively, and in some circumstances their

uncoated surfaces are contaminated by adventitious contact with fission or corrosion products as the result of leaking or spilling of liquids [1]. Concrete, that accounts for up to eighty percent of the total mass of materials present in a nuclear facility [2], is used for several purposes: as a biological shielding against the neutron flux; as a shell against the falling of massive objects such as aircrafts and against the seismic risk; or for the building of the containment enclosure walls and floor that isolates a pressurized water reactor. Thus, during disassembling and dismantling operations, hundred thousand of tons of concrete containing radioactivity over a greater or lesser thickness are handled [3]. Experimental data reveal that radioactivity is present in one to ten percent of the whole concrete mass and penetrates through several centimeters depth [4]. Accordingly, the concrete structures of nuclear installations must be sanitized so that the waste resulting from the dismantling operations meets the criterion of very low level waste (VLLW) and be storable or recyclable without any radiological restriction. Indeed, any dismantling strategy should focus on minimizing the waste volume to be handle. For instance, if a whole building containing radioactivity is demolished using explosives, all the debris is considered hazardous and need careful handling. This also means cost for surveillance and maintenance. Using a surface removal technique is more cost effective since the volume of radioactive material is limited to the removed surface thickness. Additionally, the resultant concrete conventional waste –of high quality- can be used in civil engineering sites such as road or bridge constructions depending on country specific regulations.

Concrete remediation commonly involves mechanical removal of the layer containing the radioactivity by means of various techniques (abrasive blasting, scarifying, hammering, sawing, etc.) depending on the thickness to be chopped off [5]. The stress energy of these mechanical ablation processes fragments the concrete, which unavoidably produces airborne particulate matter. The particulates in the conventional respirable and thoracic size ranges are hazardous for people who could intake them and this threat is exacerbated in presence of radioactivity. Therefore, prior to remediation and dismantling of concrete structures, it is crucial to have a good knowledge of the neutron activation and contamination they have received during their operating time and, which is leftover after shutdown, as well as the concerned thickness. This would permit to tailor the most appropriate surface treatment method (robot, operators, tools, etc.), but also to contrivance appropriate radiation protection procedures. In this regard, the French Nuclear Safety Authority (ASN) has made available a guide entitled " Complete post-operational clean out methodologies acceptable in basic nuclear installations in France [6]", where it described several recommendations on the classification surfaces containing radioactivity to be sanitized, the type of treatment to be considered depending on the activation or the contamination depth, as well as the radiological survey to be carried out after the remediation on the cleaned structures and on the produced conventional waste. Nevertheless, ASN does not provide any information about the menace associated with the resuspension of particulate matter throughout remediation operations. Indeed, various ways for assessing radioactivity levels in activated and contaminated concrete structures exist and are based on measurements of surface mass activity and radiation level on the tainted thickness [7]. Similarly, there is a plethora of studies on the formulation of internal doses and health risks related to radionuclides inhalation or ingested into human body [8],

with elaborated models combining the number of inhaled particles, tidal volume, respiratory rate, duration of exposure, etc. [9,10].

Paradoxically enough, the level of understanding of the airborne fraction mobilized from a concrete surface during remediation operations, and which makes it possible to evaluate the probability of a person to come into contact with radioactive particles, is limited. In the nuclear industry, the Brunskill [11] works provide resuspension coefficients of particulate contaminants on concrete surfaces, but these are labile contaminations deposited on concreted soils, in the form of aerosols or dried liquids which are re-suspended afterward. The study that seems the most relevant to the problematic of interest is probably that of Jardine and co-workers [12] who measured resuspension coefficients, in laboratory conditions, during the fragmentation of brittle materials (ceramic, glass and concrete) following the impact of a weight falling from a given height. They estimated a resuspended fraction of 4.3×10^{-2} on a concrete surface receiving an impact energy density of 10 J.cm^{-3}. In civil (non-nuclear) facilities, studies on the emission of particulate matter following concrete cutting operations are limited to dust monitoring, for the sole aim to tackle concerns about air quality, pollution level standards or dealing with workers occupational exposure [13, 14]. In fact, regarding nuclear safety, the interesting parameter is the ratio between the airborne contamination and the potentially dispersible amount of contamination; expressed, for the aerosol particles, in terms of airborne release fraction or rate [15, 16]. Moreover, the characteristics of the whole airborne aerosol (including non-radioactive particles) is as important as that of the radioactive particles alone regarding the safety concerns, since it determines the way the filtration and collection techniques are designed to ensure efficient confinement regarding filters clogging issues. Notwithstanding, the poverty of data on particles resuspension during concrete mechanical ablation contrasts with the abundance of studies on particles resuspension on other types of contaminated materials [15, 17,18]. Sehmel [16] has compiled nearly a hundred measurements of particle resuspension factors (ratio between air volume and surface concentration of a particulate contaminant) in indoor and outdoor environments, on surfaces contaminated mostly by radioactivity and subjected to mechanical stresses such as walking operators, cleaning activities, tilling, wind erosion, car traffic, etc. and, the documented resuspension factors extent to no less than nine decades. Hence, it would be unrealistic to draw a generic resuspension factor from these studies that would be transposable to the dismantling of concrete in nuclear facilities, even though a factor generally below 10^{-6} m^{-1} is generally considered in radiation protection procedures [19]. Moreover, it should be noticed that the resuspension factor depends on the particulate source term and also on the airflow environment influencing particles dilution, transport and deposition. Consequently, it is more convenient to assess separately the particle source term based on a release fraction or rate and the particles behavior (dilution, transport and deposition).

The glaring lack of data has motivated the launch of a dedicated experimental study on particle airborne release fraction during concrete scarifying operations, by quantifying the total amount of emitted aerosol using high volume samplers along with particle size distribution analyzing tools. It is noteworthy to mention that the work is realized in absence of radioactivity but the outcomes should be conveniently applicable to concrete structures in nuclear installations, exposed to neutron flux. Indeed, activation of concrete is rather ubiquitous and homogeneously distributed within the stricken thickness. For this, a major

activation product worthy of interest is calcium, due to its large quantity in the concrete cement [20] and the long half-life of the isotope [41] Ca of 102,000 years resulting from the [40] Ca activation. Concrete samples taken from the biological shield of two research reactors, several years after shutdown, reveal a mass activity concentration for [41]Ca of 27 Bq/g [21, 22]. Other activation products such as europium ([152] Eu and [154] Eu), Barium ([133] Ba) or tritium (^{3}H) [1, 23,] are also overseen during dismantling because of their presence, sometimes in trace amount, in concrete manufacturing material. In this respect, a mineralogical analysis on the collected particles is realized with a particular emphasis on potential activation products. As far as contamination is concerned, it occurs mostly in absence of surface coating and is thus a less widespread phenomenon. Therewith, it is confined inside cracks, which is trickier to assess in terms of resuspension fraction. Nevertheless, the radiological risks associated with concrete surface contamination cannot be overlooked regarding aged and degraded surface coatings for which the contamination barriers can be perforated.

2 - Material and method

- *The concrete slab*

A concrete slab of 2.50 m (L), 2.10 m (W) and 0.20 m (H), made of sand, gravel, cement and water mix with respect to the specifications described in Table 1 and supported with a reinforcing steel mesh, was specially poured for the purpose of the experiments. The slab was molded following the compressive strength C25/30 meeting the requirements of NF EN 12390-3 standard. This compressive strength is evaluated after loading a 28 days old specimen to failure in a compression machine. The measured density of the tested specimen is 2241 kg/m^3.
The concrete slab dried for six weeks prior to the scarifying operations.

Table 1- Composition of the C25/30 concrete slab

	Sand	Gravel	Cement	Water
Granulates	0/6.3 mm	4/14 mm	-	-
Petrography	Mixed	Alluvial	-	-
Elaboration	Semi Crushed Washed	Semi Crushed Washed	-	-
Supplier	CEMEX Granulats	LAFARGE France	CALCIA	Tap water
Place of production	Quarry of Bouafles, France	Quarry of La Brosse Montceaux, France	Couvrot plant, France	Champ sur Marne, France
Standard	XPP 18-545	NF P 18-545	CEM II / B-LL 32.5R	-

Quantity (kg per m³ of C25/30)	982	814	410	245

- *The cement composition*

Clinker is the main constituent of cement fabrication. It is obtained by cooking at 1450 ° C a mixture of limestone (calcium carbonate) and clay (aluminum silicate) (~2/3 limestone and ~1/3 clay). Note that these proportions do not follow any standard and are as a matter of fact only indicative.

- *The industrial milling machine*

The scarifying operations were accomplished using a manually propelled industrial milling machine (Blastrac BMP-265E) of 175 kg, powered by an electric motor at 5.5 kW. The machine works with milling cutters arranged all around a rotatable drum spinning at 1500 rpm, enclosed in a containment shelter and plumbed in a vacuum dust collector (BDC138-HLP) positioned outside the tent, that is equipped with a HEPA certified bagging system (Figure 1). An aspiration flowrate of 2.45 m³/min was estimated by a hot wire anemometer probe measuring close to the drum center, knowing the shelter section.
The machine weight is centered on the drum that is sited on the concrete slab. The milling machine works with adjustable depths.

Figure 1 - The Blastrac milling machine equipped with a tubing sitting on the concrete slab (left) and the vacuum dust collector with its bagging system

- *The experimental chamber*

The study was performed in a closed experimental tent, stretched on an inflated skeleton, in the shape of a half elliptic cylinder (Figure 2). The tent volume can be approximated using the expression $V = \frac{1}{4}\pi R r L$, with R (m) the height of the tent, r (m) its width and L (m) its length. Accordingly, the outside volume is ~ 101 m^3 but the inside volume is tricky to estimate because it requires subtracting the volume of the inflated skeleton which is in the form of mesh with voids. In the hypothesis of a fully filled tent frame, this volume would be ~ 57 m^3. A different way of evaluating the tent true volume is based on the "closed box" method presented in appendix A. Knowing the air cleaning characteristic time of the tent and the total ventilation flowrate, the volume is ~97 m^3. This value is closer to the outside volume.
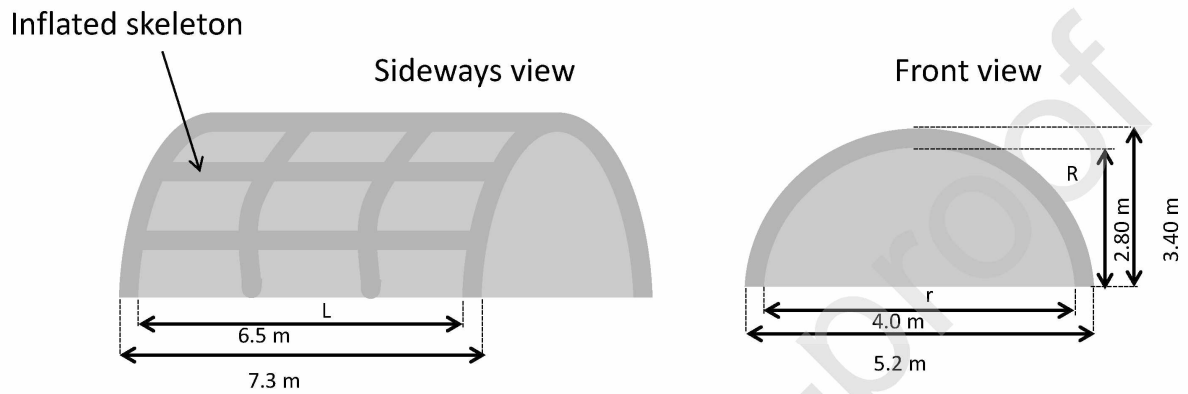
Figure 2 - Schematic representation of the experimental tent

- *The aerosol collection system*

During the scarifying operations, the aerosol number concentration and the size distribution in the tent were monitored in real time by an optical particle counter (Grimm 1.109) over a time step of 6 s. The particle mass size distribution was also assessed using a more straightforward method by an Andersen Cascade Impactor (ACI) that gives access to particles aerodynamic equivalent diameter.

The emitted aerosol was collected by five high-volume samplers (HVS-TSP) working at 1.13 m^3/min flowrate on HEPA (High Efficiency Particulate Air) filters with no preference to size selection and with sampling efficiency close to 100 % for particle aerodynamic diameters below 5 μm and low wind velocity conditions [24, 25]. To maintain a constant sampling flowrate during operation, a hot wire anemometer probe inserted into the flow stream automatically adjusts the motor speed as the HVS-TSP filter begins to collect significant amount of particles and causes pressure drop increase. The schematic of HVS samplers implantation inside the tent is shown in Figure 3.
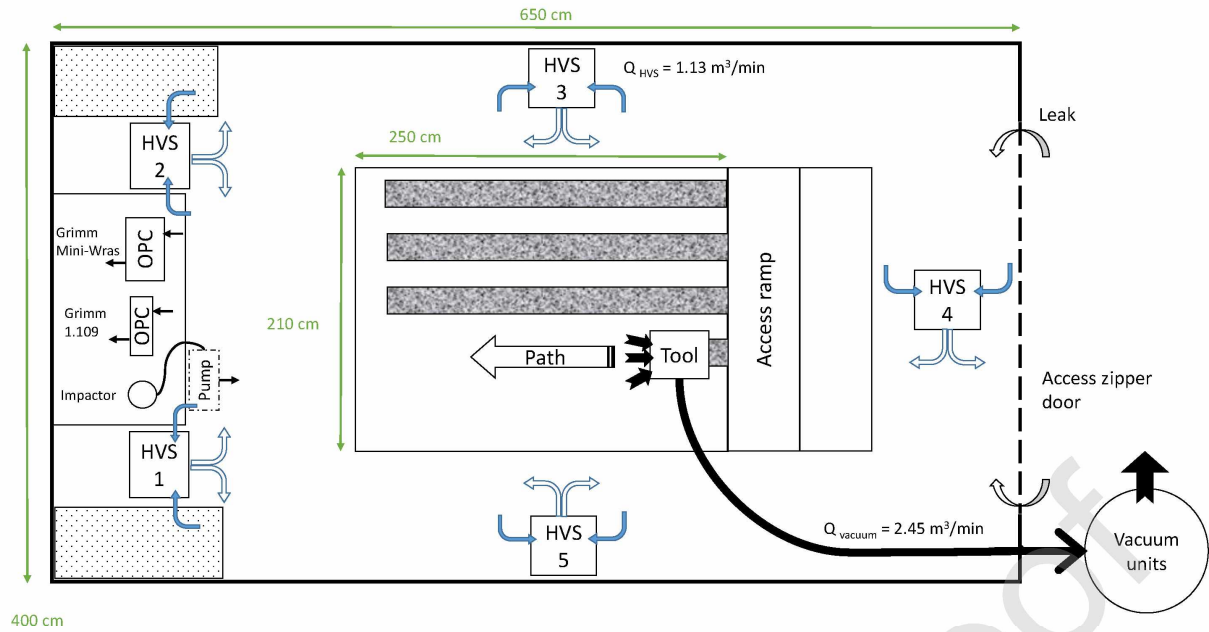
Figure 3- Schematic representation of the experimental setup

3 - Results

- *Dust concentration*

Prior to scarifying operations and in-between trials, the experimental tent was wiped up and the absence of background dust established by the absence of particles in a detectable amount on the HVS-TSP filters - sampled for half an hour- by double weighing. This procedure guarantees that the generated airborne particles come exclusively from the milling. The temperature and relative humidity recorded in the tent during trials were between 25°C and 30° C and 40 % and 45 %, respectively.

The scarifying was done on one-way rides, on a working width of 265 mm until a working depth of about 10 mm was reached over the slab length, after more or less 8 runs, during a period less than 10 minutes. All through the milling phase, an abrupt rise of aerosol concentration is observed inside the tent that results in a quick decline of visibility (Figure 4 - see also supplementary video).

Figure 4 - Dust perceptible to the naked eyes along with a milling ride; on the back right, the connecting pipe to the vacuum is distinguishable

Dust production in a significant amount is evidenced by the Grimm 1.109 optical particle counter monitoring, which exhibits an increase in aerosol concentration. This is because the aerosol production rate in the tent is greater than that of their disappearance by aspiration on the HVS filters and the vacuum mitigation system. Once the scarifying operation is completed, there is no more aerosol source and consequently the aerosol concentration decreases rather exponentially over time (Figure 5). The milling operation is clearly accompanied by the production of substantial quantity of aerosol, even though the dust production is mitigated by a vacuum system; the maximum particle number concentration C_{max} being ~2.8×10^9 #/m^3. About one hour after the ending of the milling, the dust particles are all collected and the aerosol concentration goes back to the background value.
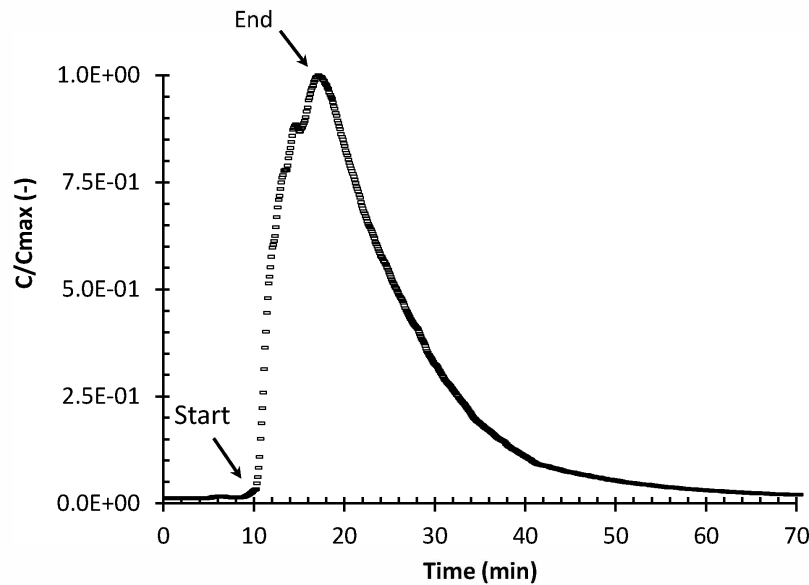
Figure 5 - Evolution of the aerosol concentration inside the experimental tent during a milling operation trial. The concentration is normalized to the maximum value

- *Particle size distribution*

The airborne particle size distribution (PSD) was assessed throughout the milling operation trials with two different means: as equivalent optical diameter form the Grimm optical particle counter (OPC) and as aerodynamic equivalent diameter from the Andersen cascade impactor (ACI).

The OPC detects scattered laser-light in 15 size channels: [> 0.30 µm]; [> 0.40 µm]; [> 0.50 µm]; [> 0.65 µm]; [> 0.80 µm]; [> 1.0 µm]; [>1.6 µm]; [> 2.0 µm]; [> 3.0 µm]; [> 4.0 µm]; [> 5.0 µm]; [> 7.5 µm]; [> 10.0 µm]; [> 15.0 µm] and [> 20.0 µm]. The Grimm 1.109 OPC assesses the PSD indirectly by comparing the electronic pulse strength of the scattering particle to the one of a size-calibrated spherical latex particle. The raw PSD from the OPC is presented in the form of a cumulative count fraction. Assuming spherical particles and ignoring the particles refractive index bias, we make an estimation of the PSD in terms of particles volume (or mass) which gives access to the mass median diameter (MMD) (half of the particles have a diameter less than the MMD). The MMD given by optical particle sizing is between ~4 and 5 µm (fig. 6).

The Andersen cascade impactor with 8 collection stages has channels with aerodynamic cutoff sizes: [> 9 µm]; [> 5.8 µm], [> 4.7 µm]; [> 3.3 µm]; [> 2.1 µm]; [> 1.1 µm]; [> 0.7 µm] and [> 0.4 µm], respectively. The PSD evaluation with the ACI is more straightforward since each stage separates aerosol particles into two size ranges. Particles larger than the cutoff size are removed from the aerosol stream and are collected on a substrate for weighing; particles smaller than that size remain airborne and pass through the next stages and so forth. The aerosol mass collected on the different ACI collection stages (fiberglass filters are used as collection substrate) were: 1.7 mg; 4.1 mg; 3.8 mg; 6.4 mg; 3.6 mg; 1.7 mg; 0.2 mg and 0.2 mg, respectively. The mass median aerodynamic diameter (MMAD) of the PSD obtained with

9

the ACI is 4.3 µm with a geometric standard deviation (GSD) equal to 1.7 as represented on figure 6.
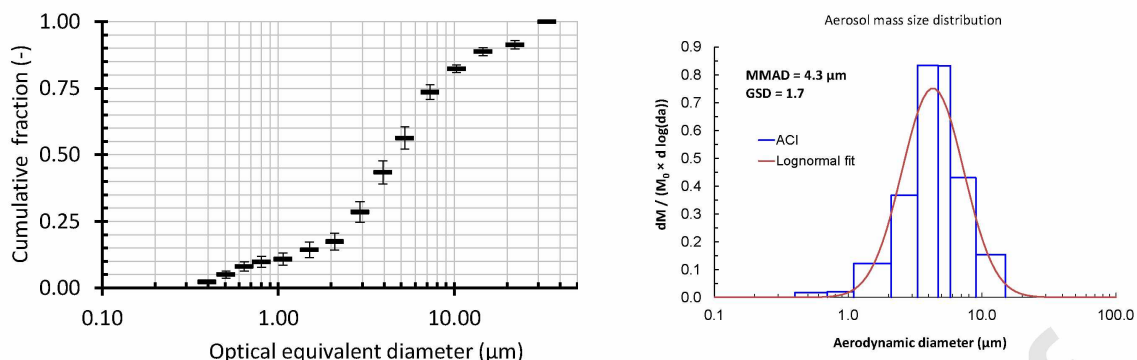

Figure 6 - Particle size distribution expressed as optical equivalent diameter from the OPC (left) and as aerodynamic diameter from the ACI (right) for a milling operation trial

To extend further the aerosol release fraction size analysis, the PSD of the dust collected either in the vacuum bag or scrubbed from the HVS-TSP filters was assessed as aerodynamic diameter from time-of-flight analysis (PSD 3603 Particle Size Distribution Analyzer, TSI). The PSD 3603 analyzer disperses and accelerates individual particles through two laser beams. As the particles passes through the laser beams, a detector records the scattered light that is converted to an electric pulse. The passage time between the two beams, called the time-of-flight, is measured and transformed to an aerodynamic equivalent diameter by a reference table, done by calibration with size-calibrated spherical particles. The volume and number PSDs obtained using this technique are shown in figure 7. In the figure representing the particle number size distribution (on the right), the result obtained on reference particles made out of standard glass bead whose average diameter is 2.5 µm is also shown. Analyzes performed with the PSD 3603 show that the particles collected by the HVS and by the confinement vacuum bag have quite similar size modes around 1 µm to 2 µm. On the other hand, the volume (mass) particle sizes measured by the PSD 3603 reveal that the distribution is bimodal with a mode for large particles at about 20 µm. This later mode could be related the handling of the scrubbed dust that can lead to the formation of aggregates due to the inter-particle adhesion forces (van der Waals, electrostatic). These aggregates are not necessarily well deagglomerated by the powder disperser of the PSD 3603 instrument. Therefore, we do not think that the coarse mode is representative of the airborne particles. To support this assumption, we assessed the sampling efficiency of the Andersen impactor inlet with the model developed by Grinshpun et al. 1993 26[26] in order to verify the ability of the instrument to catch such coarse particles. If it is assumed that the impactor samples the aerosol in an atmosphere with slow moving airflow and with a horizontal velocity below 0.5 m/s (which is a reasonable hypothesis in our experimental configuration) the sampling efficiency of the impactor inlet is above 80 % for particles with aerodynamic diameters below 35 µm.

Regarding the volume distribution mode for particles smaller than 10 μm, it is found that the one determined by the PSD 3603, between 2 and 3 μm, is noticeably smaller than that determined by the ACI. Indeed, several studies have shown that the PSD 3603 underestimate the size of particles by 20 to 50 % when they are not perfectly spherical [27]. Therefore, the PSD 3603 measurements can be arguably considered to be consistent with the other PSD analysis methods.
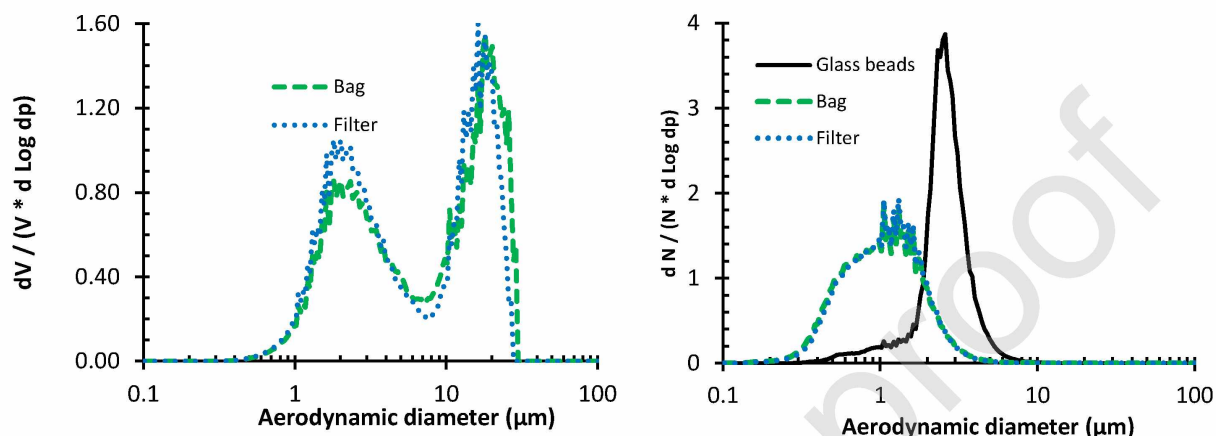

Figure 7 - Volume particle size distributions (left) and number (right) of particulates taken from one of the HVS filters and the vacuum bag filter

The results on the PSD of airborne particles produced during the scarification operation from the impactor measurement taken as reference are in the micron size range. Consequently, it is relevant to assess the different conventional size fractions [28] for this type of aerosol as defined for occupational worker exposure assessment.

These particle size-selective fractions called: inhalable (the aerosol fraction which enters the nose and/or the mouth during breathing), thoracic (the sub fraction of inhalable aerosol which penetrates into the respiratory tract below the larynx) and respirable (the sub fraction of inhalable aerosol that penetrates down to the alveolar region of the lung). These fractions are represented in the form of curves (fig. 8, curves fraction in terms of *penetration probability in airways*), which relate the probability of inhalation, or penetration to the thoracic or alveolar regions, as functions of particle aerodynamic diameter. The standardized functions used to compute these curves are detailed in references [26], [29], and [30].

These curves are a guidance to design a specific aerosol samplers and to operate the particle sampling in order to get directly representative particle concentrations that could reach the three regions in the basis of occupational worker exposure. For that purpose, we determine the three conventional fractions corresponding to the aerosol PSD measured with the ACI. For more convenient calculations, we used a lognormal fit of PSD (represented by the blue line in fig. 8 in terms of *normalized particle size fraction*).

The three conventional fractions specific to the aerosol PSD are obtained by multiplying the penetration probability by the normalized particle size fraction and integration over the

particles size spectrum. Values equal to 88 %, 82 % and 45 % are obtained respectively for inhalable, thoracic and respirable fractions. This means, as an example, that 45 % of the ambient aerosol mass concentration could penetrate to the alveolar region of an operator. The high values obtained (i.e. > 80 %) for inhalable and thoracic fractions make sense since the aerosol PSD measured with ACI exhibit mainly particles with aerodynamic diameters below 9 μm, for which inhalation probability and penetration to thoracic region is higher than 50 %.
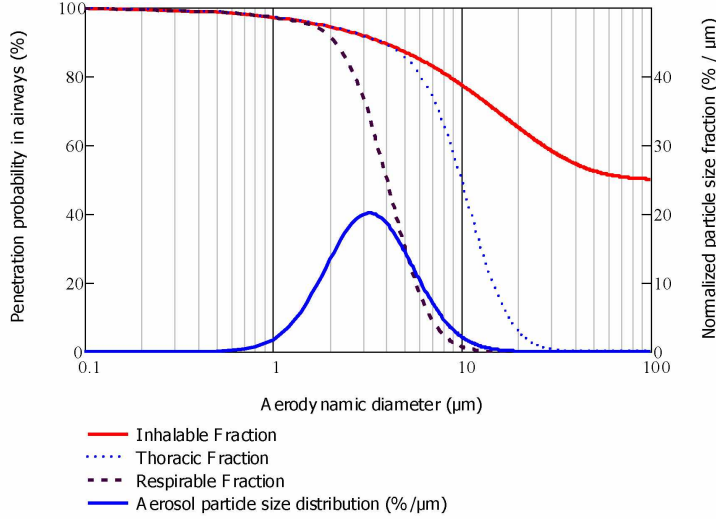

Figure 8 – Conventional particle size fractions compared to particle size distribution measured by the ACI and considered as lognormally distributed

- *The aerosol release fraction*

To appropriately evaluate the aerosol release fraction (ARF), it is mandatory to verify that the produced airborne particles are homogenized in the experimental enclosure and can be collected by the HVS samplers. It is worth mentioning that the experiments were done without a dedicated ventilation system; nevertheless, the high volume samplers, that have the specificity of sucking and exhausting the air within the tent, generates an air cleaning process. The homogeneity of the aerosol in the experimental tent has been verified using a "closed box" method by monitoring the aerosol concentration over time (Appendix A). The calculations reveal a quasi-homogenous air mixing in the tent during the milling trials.

The raw ARF is expressed as the ratio of the aerosol mass collected on the HVS-TSP filters and the whole mass of concrete scarified:

$$ARF(-) = \frac{mass\ of\ collected\ aerosol\ (kg)}{mass\ of\ scarified\ concrete\ (kg)}. \tag{1}$$

The quantity in the numerator of eq. 1 is assessed by differential weighing of the HVS-TSP filters and totaling the mass collected over the five filters. Note that the OPC (5 L/min) and the ACI (28 L/min) operate at a low flowrate, several orders of magnitude smaller than the HVS-TSP (5×1.13 m³/min). The quantity on the denominator is evaluated with two different

methods: 1) by collecting and weighing the gravels on the concrete slab that are too heavy to be pumped out to the vacuum bag and the ones that have rolled underneath the ramp supporting the slab, then to this mass is added the mass of dust collected in the vacuum bag itself; 2) by evaluating the chopped off volume of concrete - using a sliding caliper for the thickness and a ruler for the length and the width- which is multiplied with concrete density (Figure 9).
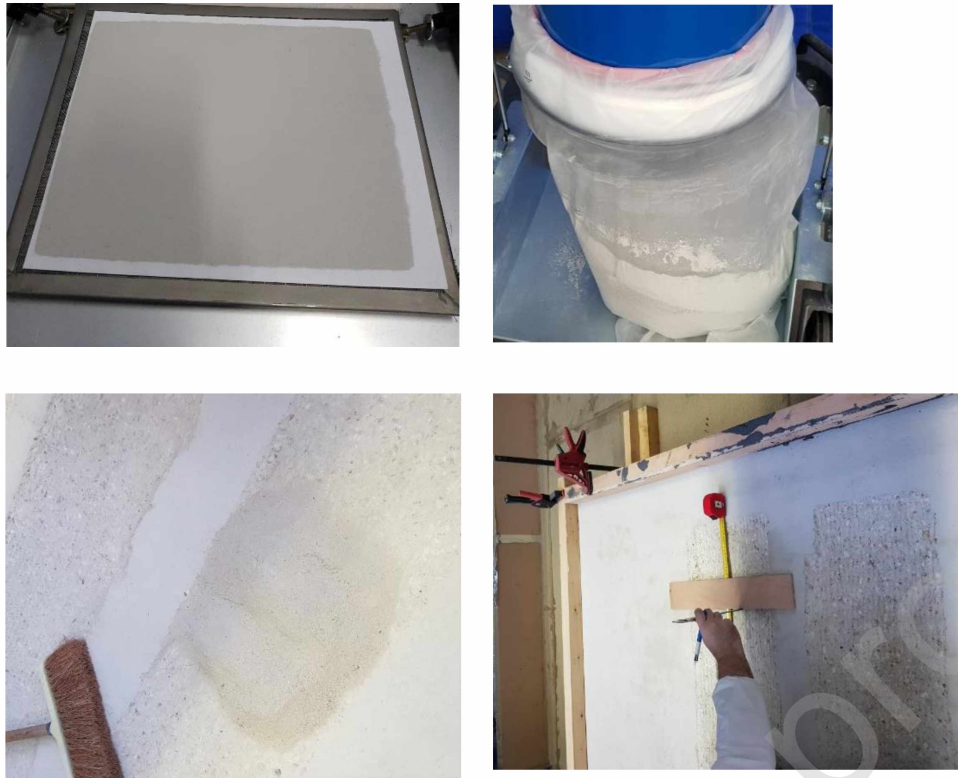
Figure 9 - Top left) aerosol collected on a HVS-TSP filter, top right) dust pumped off
to the vacuum collecting bag, bottom left) heavy gravels scrubbed on the concrete slab
and bottom right) chopped off concrete volume measuring.

Table 2 presents the recorded values from one milling operation trial. The collected mass of
aerosol is in the order of magnitude of one gram per filter with a quite balanced distribution
on the different HVS-TSP samplers, which is another good indication of the air aerosol
mixture homogeneity in the tent. The mass of removed concrete is in the order of a few
kilograms with about half of this mass in the vacuum collecting bag. The mass of scarified
concrete (mass losses of the slab), assessed either with the weighing of the rubble plus dust in
the vacuum bag or with the lost volume calculation, is quite consistent with a mass of about
17 kg for each trial and about 5 % difference for the three trials.

Table 2 - Measured airborne and bulk concrete mass during a milling trial

Mass of aerosol collected (g)		Mass of scarified concrete (kg)		Estimated mass of scarified concrete (kg)	
HVS 1	1.23 (g)	Inside the vacuum bag	8.87 (kg)	Tickness	1.33 (cm)
HVS 2	1.20 (g)	On top of the slab	5.58 (kg)	Length	26.5 (cm)
HVS 3	1.29 (g)	Underneath the ramp	2.72 (kg)	Width	225 (cm)
HVS 4	0.78 (g)	-	-	Volume	7930 (cm^3)
HVS 5	1.58 (g)	-	-	Density	2.214 (g/cm^3)
Total	6.09 g	17.17 kg		17.56 kg	

The ARF, for the three milling operation trials, is presented in table 3 using the weighted chopped off concrete mass, along with blank measurement before each trial, and the number of one-way milling runs during the concerned trial. The blanks are three orders of magnitude smaller than the collected mass on the HVS-TSP filters confirming that the airborne particles come exclusively from the milling operation during a trial. The mean raw ARF value is 3.09×10^{-4} with a COV of 27 % that shows a good repeatability of the measurements.

However, this raw ARF values do not take into account the fraction of released particles that were not sampled by the HVS-TSP. Indeed, during the aerosol sampling with HVS-TSP, a fraction of the airborne particles is deposited by settling and thus not collected. This non-collected fraction that depends on available floor surface, sampling and vacuum bag flowrates becomes important as particle size enlarges due to gravity. Thus, a loss multiplying coefficient, α, must be applied to the collected mass of aerosol to accurately evaluate the ARF source term.

The loss coefficient, which refers to an aerosol collection yield, is assessed analytically using the "closed box model". It is also validated experimentally by dispersing a calibrated mass of aerosol with a defined size distribution, in the experimental tent and measuring the mass effectively collected by the HVS-TSP samplers. This experimental validation is necessary to correctly assess the particle losses due to deposition and intrinsic sampler efficiency. The experimental results are presented in Appendix B.

Calculated value of the loss coefficient, α, is 1.59 which corresponds to an aerosol collection yield of 63 %. The mean ARF taking into account the loss coefficient is thus 4.9×10^{-4}. This value is two orders of magnitude lower than the ARF measurements found in the literature related to fragmentation of concrete surface after weight impacts [11]. This large difference could stem from the energy delivered to fragment the concrete sample in addition to the fact that the scarifying machine is equipped with a vacuum mitigation system.

It appears that the vacuum dust containment system combined to the concrete milling operation reduces significantly the dust generation but does not suppress entirely the aerosol release. Indeed, in absence of the vacuum containment, in the hypothesis that all the dust collected in the vacuum bag filter was airborne, the ARF should have been in the order of magnitude of 5×10^{-1}; which would mean that half of the mass of concrete scarified is become airborne during the milling operations. This assumption is relevant since the dust collected in the vacuum bag filter exhibit similar size distribution to the one collected by HSP-TSP samplers as shown Fig. 7.

Table 3 - The ARF assessed for three trials and its mean value

Trial	# runs	Blank (g)	Airborne (g)	Scarified (kg)	Raw ARF	ARF accounting for collection yield
1	7	0.015	6.09	16.87	3.61×10^{-4}	
2	9	0.029	5.15	14.57	3.54×10^{-4}	
3	7	0.015	3.17	15.03	2.11×10^{-4}	
Mean			4.80	15.49	3.09×10^{-4}	4.9×10^{-4}
COV			37 %	8 %	27 %	

ARF is a key parameter that is mandatory to evaluate the source term of contamination, so that the radiological consequence of an operation can by assessed by dismantling operators for normal conditions and accidental scenarios. The other important parameter is the particles size distribution (PSD) which pilot aerosol penetration in airways, efficiency of personal protective equipment and also aerosol transfer in ventilated enclosure and network down to potential exhaust to environment. ARF together with PSD are of primary interest to design containment systems based on filtration or epuration process.
ARF depend on the selected scarifying machine and whether or not it is equipped with a suction device. The concrete mechanical characteristics and ageing could also affect the ARF value. Due the variety of the available milling machines, the value of ARF determined in this study cannot therefore be generalized. Nevertheless, this first thorough study gives the order of magnitude for ARF which could be expected in concrete dismantling procedures and a detailed methodology to assess the ARF for other scarifying machine and configurations.

- *Chemical and mineralogical characterization*

The elemental and the mineralogical composition is assessed using X-ray analytical techniques to identify major and minor concrete compounds which could lead to activation products in operating nuclear facilities.

Analyses were performed on particle samples both scrubbed from the HVS filters and collected in the vacuum bag filter.

X-ray fluorescence spectrometry (XRF) is used to identify the elements present in the samples (except the elements lighter than sodium) and their proportions. In addition, the sample mineralogical composition is established using X-ray diffraction (XRD). This coupled information is necessary for the characterization of the dust elemental compounds as well as their oxidized form.

The bulk elemental composition analysis on the dust samples is done using XRF — Epsilon 3XL, Panalytical spectrometer — that identifies chemical elements from sodium to uranium and quantify them (for mass concentrations ranging from a few ppm to several tens of percent). For accurate XRF analysis of the major elements (Si, Al, Na, Mg, Ca, K, P, Mn, Fe, Ti), the samples are prepared with the fusion bead method using an automatic beader — LENeo Claisse —. This eliminates heterogeneity due to grain size and matrix effects (secondary excitation of the lightest elements) since the samples are diluted.

Table 4 (dust on filters extracted by ethanol ultrasonic bath) and Table 5 (dust in the vacuum bags) depict the weight percentage of the elements obtained by summing all the elemental masses converted into their most common oxides. The presented results are the mean values for three repetitions and their standard deviation. Table 4 presents the analysis on five filters from one milling trial while in table 5 the dust particles collected in vacuum bag for two different trials are examined.

The results show that calcium and silicon are in prevalent quantities in the dust samples along with some elements in small amount such as aluminum and sodium. The preponderance of calcium (about 70 %) and silica (about 18 % to 27 %) on the HVS filters and in the vacuum bags is not surprising due to the presence of calcium carbonate and aluminum silicates in the concrete cement; furthermore, quartz (SiO_2) is the main mineral in sand and gravels to some extent. Nevertheless, the evaluation of their quantitative portions in the dust mass is valuable since it is not obtainable from the concrete fabrication specifications.

Table 4 - Elemental ratios characteristic of dust from the HVS-TSP filters

	Filter 1		Filter 2		Filter 3		Filter 4		Filter 5	
	Weight (%)	σ	Weight (%)	σ	Weight (%)	σ	Weight (%)	σ	Weight (%)	σ
Na2O	1.82	0.13	1.55	0.24	1.09	0.16	1.78	0.12	0.73	0.09
MgO	0.19	0.10	0.23	0.03	0.25	0.03	0.20	0.00	0.21	0.06
Al2O3	3.42	0.07	2.86	0.01	2.94	0.03	3.49	0.04	2.62	0.04
SiO2	21.81	0.36	20.82	0.18	18.98	0.12	22.27	0.01	17.91	0.06
P2O5	0.08	0.02	0.07	0.01	0.08	0.02	0.08	0.01	0.07	0.01
K2O	0.85	0.01	0.82	0.01	0.70	0.01	0.86	0.01	0.63	0.00
CaCO3	70.42	1.01	72.25	0.46	74.63	0.65	69.89	0.09	76.53	0.41
TiO2	0.44	0.01	0.39	0.00	0.29	0.00	0.45	0.00	0.24	0.00
MnO	0.03	0.00	0.03	0.00	0.03	0.00	0.03	0.00	0.03	0.00
Fe2O3	0.94	0.01	0.97	0.01	1.00	0.01	0.95	0.00	1.03	0.00

Table 5 - Elemental ratios characteristic of dust from the vacuum bag filter

	Bag 1 Mean	σ	Bag 2 Mean	σ
Na_2O	0.10	0.01	0.22	0.01
MgO	0.23	0.04	0.31	0.03
Al_2O_3	2.49	0.05	2.36	0.06
SiO_2	26.92	0.11	27.42	0.13
P_2O_5	0.08	0.02	0.09	0.01
K_2O	0.73	0.00	0.71	0.00
$CaCO_3$	68.41	0.42	67.55	0.38
TiO_2	0.10	0.00	0.10	0.00
MnO	0.03	0.00	0.03	0.00
Fe_2O_3	0.91	0.51	1.21	0.01

The mineralogical composition is determined using a XRD — Panalytical Diffractometer — that assesses the crystals structure present in a given sample and which is capable of identifying not only the elemental minerals but also evaluating the proportions of each of their mineralogical phase.

XRD indicates the presence of calcium carbonate and silicon oxide in dominant quantity on the concrete dust samples from both the filters and the vacuum bags (see table 6), which is consistent with the XRF analysis. Other minerals in fewer proportions such as calcium hydroxide (Portlandite), a byproduct of concrete cement hydration, are also present.

Table 6 - Mineralogical ratios characteristic of the dust from the filters and the vacuum bags

Mineral	Quartz SiO_2	Calcite $CaCO_3$	Portlandite H_2CaO_2	Andradite $Ca_3Fe_2O_{12}Si_3$	Apatite $Ca_5(PO_4)_3(OH, Cl, F)$	Bernalite $FeO_3.25H3.5$	Rutile TiO_2
Filter	12.7	79.4	3.3	0.1	-	2.7	0.2
Bag	25	68.9	2.7	-	2.6	-	0.8

A more careful examination of both XRF and XRD analysis suggests a slight enrichment in calcium within the dust particles collected on the HVS filters compared to the ones in the vacuum bag filters. XRF shows a higher Ca/Si ratio of ~3.7 on the HVS filters against 2.5 in the vacuum bag filters XRF. This Ca/Si ratio difference is even exacerbated looking at XRD to 6.2 against 2.8, for the dust from the filters and the bags respectively. This latter observation can somewhat be related to part of the silica being in an amorphous form, thus not detectable by XRD that is only sensitive to crystal structure. The calcium enrichment (or silicon depletion) on the dust collected from the HVS filters is qualitatively investigated further by scanning electronic microscopy (SEM) image analysis. As shown in figure 10, the

dust from the filters (left) exhibits particles mainly in form of small aggregates, while the dust from the bags (right) reveals the presence of larger fragments along with the aggregate. Energy Dispersive X-Ray (EDX) characterizations, integrated to the SEM apparatus, reveal higher calcium contents on the aggregate and higher silicon contents on the larger fragments.

The hypothesis that can be put forward to explain the calcium enrichment on the HVS-TSP filters may be related to the difference in mineral hardness between calcium carbonate and silicon oxide that could promote calcium fragmentation. More specifically, calcium carbonate that is at the magnitude of 3 in the Mohs scale of mineral hardness, against 7 for silicon oxide, should require less breakup energy from the milling machine.
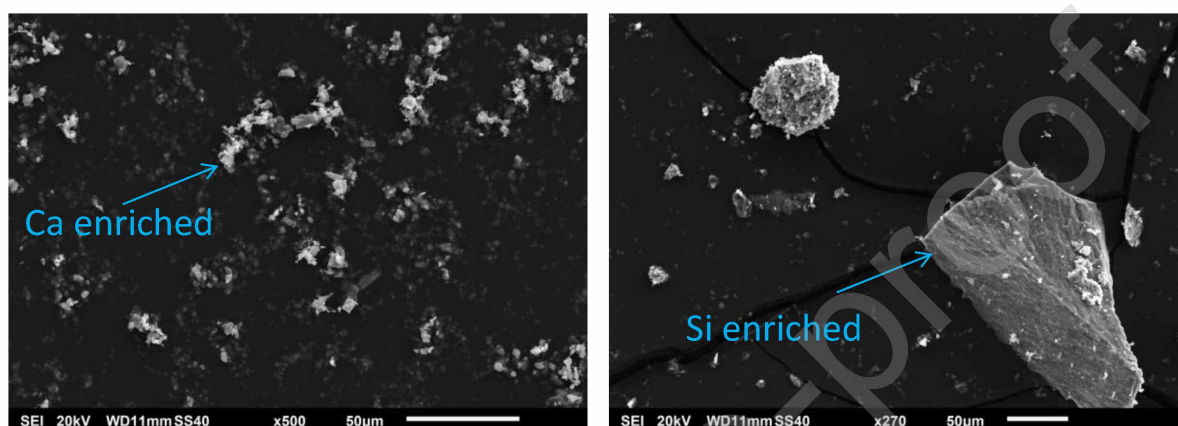

Figure 10 - SEM image of concrete dust particles scrubbed from the HVS-TSP filters (left) and collected from the vacuum bag (right)

In absolute terms, the chemical and mineralogical analysis of particles collected either on the HVS-TSP filters or in the vacuum bag filter points out the presence of calcium, which is a major concrete activation product, in dominant quantity in the dust samples collected either on the HVS-TSP filters or in the vacuum bag filter. Indeed, calcium has a particular radiological concern because of the very long half-life period of ^{41}Ca nuclide, estimated at 102 000 years. It is produced by the ^{40}Ca (n, γ) ^{41}Ca activation reaction from the ^{40}Ca stable isotope.

The detailed physical and chemical characterization on the non-radioactive particulate matter studied here gives basics data needed to make transposition to radiological studies taking into account specific activation scenarios of elemental compounds in nuclear concrete.

4 - Conclusions

We carried out experimental study on dust airborne release fraction during concrete milling procedures to investigate the level of contamination to which operators could be exposed through dismantling in nuclear facilities. The work is relevant for aerosol release associated with activated concrete structure exposed to neutron flux rather than surface contamination due to absence or damaged coating layers. The milling operation completed on a standard

19

non-radioactive concrete slab was accompanied by the production of significant airborne dust even though the dust release is mitigated by a vacuum system. The results show that the typical size distribution of the aerosol produced during the scarifying operations in this study have a mass median aerodynamic diameter equal to 4.3 μm with a geometrical standard deviation of 1.7. For this aerosol size distribution, the respirable conventional fraction is 45 % and the thoracic conventional fraction is 82 % of the ambient concentration. The mineralogical composition of particles is dominated by calcium carbonate which gives long-lived activation product. The mean airborne release fraction (ARF) determined from the experiments is 4.9×10^{-4}. Moreover, the vacuum system connected to scarifying machine helps reduce the aerosol release but does not suppress it entirely. The ARF estimated from the dust mass accumulated in the vacuum bag filter would have been around 5×10^{-1} without the vacuum containment device. Hence, during mechanical sanitizing of activated concrete structures, the radiological impact of fine dust bearing long-lived calcium nuclide cannot be overlooked.

Declaration of interests

The authors declare that they have no known competing financial interests or personal relationships that could have appeared to influence the work reported in this paper.

Credit Author Statement
The submission of the manuscript has been approved by all co-authors.

References

[1] IAEA (1998). Radiological Characterization of Shut Down Nuclear Reactors for Decommissioning Purposes. *Technical Reports Series No. 389*. IAEA, Vienna.

[2] Anigstein, R., Chmelynski, H. J., Loomis, D. A., Marschke, S. F., Mauro, J. J., Olsher, R. H., Thurber, W. C., & Meck, R. A. (2004). Radiological assessments for clearance of materials from nuclear facilities. *NUREG-1640, Vol. 2*. Division of Systems Analysis and Regulatory Effectiveness, Office of Nuclear Regulatory Research, US Nuclear Regulatory Commission.

[3] Haristoy, D., Guetat, P., & Chapuis, A. M. (1995). Définition des autorisations de sortie ou clearance levels pour les bétons venant du démantèlement. *Rapport EUR 16004 FR*.

[4] Smith, G. M., Hemming, C. R., Clark, J. M., Chapuis, A. M., & Garbay, H. (1985). Methodology for evaluating radiological consequences of the management of very low-level solid waste arising from decommissioning of nuclear power plants. *Commission of the European Communities*.

[5] O'Sullivan, P., Nokhamzon, J. G., & Cantrel, E. (2010). Decontamination and dismantling of radioactive concrete structures. *NEA News*, 28(2), 27-29.

[6] Autorité de Sûreté Nucléaire, (2010). Complete post-operational clean out methodologies acceptable in basic nuclear installations in France. *ASN guide n° 14*.

[7] Angus, M. J., Hunter, S. R., & Ketchen, J. (1990). Classification of contaminated and neutron-activated concretes from nuclear facilities prior to their decontamination or decommissioning (*No. CONF-900210--VOL. 2*).

[8] Majid, A. A., Ismail, A. F., Yasir, M. S., Yahaya, R., & Bahari, I. (2013). Radiological dose assessment of naturally occurring radioactive materials in concrete building materials. *Journal of Radioanalytical and Nuclear Chemistry*, 297(2), 277-284.

[9] Bailey, M. R., & Puncher, M. (2007). Uncertainty Analysis of the ICRP Human Respiratory Tract Model Applied to Interpretation of Bioassay Data for Depleted Uranium. *Health Protection Agency, Radiation Protection Division*.

[10] Eckerman, K., Harrison, J., Menzel, H. G., & Clement, C. H. (2012). ICRP publication 119: compendium of dose coefficients based on ICRP publication 60. *Annals of the ICRP*, 41, 1-130.

[11] Brunskill, R. T. (1967). The relationship between surface and airborne contamination. *In Surface Contamination, Proceedings of a Symposium Held at Gatlinburg, Tennessee (pp. 93-105). Pergamon Press*.

[12] Jardine, L. J., Mecham, W. J., Reedy, G. T., & Steindler, M. J. (1982). *Final report of experimental laboratory-scale brittle fracture studies of glasses and ceramics* (No. ANL--82-39). Argonne National Lab..

[13] Azarmi, F., Kumar, P., & Mulheron, M. (2014). The exposure to coarse, fine and ultrafine particle emissions from concrete mixing, drilling and cutting activities. *Journal of hazardous materials*, 279, 268-279.

[14] Kumar, P., Mulheron, M., & Som, C. (2012). Release of ultrafine particles from three simulated building processes. *Journal of Nanoparticle Research*, 14(4), 1-14.

[15] DOE-HDBK-3010-94 December 1994 Reaffirmed 2013. Airborne release fractions/rates and respirable fractions for nonreactor nuclear facilities.

[16] Nicholson, K. W. (1988). A review of particle resuspension. *Atmospheric Environment (1967)*, 22(12), 2639-2651.

[17] Sehmel, G. A. (1980). Particle resuspension: a review. *Environment International*, 4(2), 107-127.

[18] Sansone, E. B., & Slein, M. W. (1977). Redispersion of indoor surface contamination: A review. *Journal of Hazardous Materials*, 2(4), 347-361.

[19] Brodsky, A. L. L. E. N. (1980). Resuspension factors and probabilities of intake of material in process (or Is 10^{-6} a magic number in health physics'). *Health Physics*, 39(6), 992-1000.

[20] Matschei, T., Lothenbach, B., & Glasser, F. P. (2007). The role of calcium carbonate in cement hydration. *Cement and Concrete Research*, 37(4), 551-558.

[21] Hou, X. (2005). Radiochemical determination of 41Ca in nuclear reactor concrete. *Radiochimica Acta*, 93(9-10), 611-617.

[22] Itoh, M., Watanabe, K., Hatakeyama, M., & Tachibana, M. (2002). Determination of 41 Ca in biological-shield concrete by low-energy X-ray spectrometry. *Analytical and bioanalytical chemistry*, 372(4), 532-536.

[23] Evans, J.C. et al. (1984). Long-Lived Activation Products in Reactor Materials. *NUREG/CR-3474*.

[24] Krug, J.D., Dart, A., Witherspoon, C. L., Jerome Gilberry, J., Malloy, Q., Kaushik, S. & Vanderpool, R. W. (2017) Revisiting the size selective performance of EPA's high-volume total suspended particulate matter (Hi-Vol TSP) sampler, Aerosol Science and Technology, 51:7, 868-878, DOI: 10.1080/02786826.2017.1316358.

[25] Wedding, J. B., McFarland, A. R., and Cermak, J. E. (1977). Large Particle Collection Characteristics of Ambient Aerosol Samplers. Environ. Sci. Technol., 11(4):387–390.

[26] Grinshpun, S.A., Willeke, K., Kalatoor, S. (1993) A general equation for aerosol aspiration by thin-walled probes in calm and moving air. *Atmos. Envir.*, 27A, 1459-1470. Corrigendum, Atmos. Envir., 28, 375, 1994

[27] Cheng Y.S., Barr E.B., Marshall I.A., and Mitchell J.P. (1993) Calibration and performance of an API Aerosizer. *J. Aerosol Science*, **24**, 501-514.

[28] EN 481 (1993) Workplace Atmospheres - Size fraction definitions for measurement of airborne particles in the workplace. CEN, Bruxelles.

[29] ACGIH (1996) Threshold Limit Values for Chemical Substances and Physical Agents and Biological Exposure Indices. American Conference of Governmental Industrial Hygienists, ACGIH, Cincinnati, Ohio.

[30] International Organization for Standardization (ISO). (1995) Air Quality—Particle Size Fraction Definitions for Health-Related Sampling. ISO 7708:1995. ISO, Geneva.